A New Exoskeleton-type Masterarm*with Force Reflection based on the Torque Sensor Beam

Yoon Sang Kim[†], Sooyong Lee[‡], Changhyun Cho, Munsang Kim, Chong-Won Lee
Advanced Robotics Research Center
Korea Institute of Science and Technology, Seoul, Korea
`yoonsang@rcs.ee.washington.edu`

Abstract

A new concept of the exoskeleton-type masterarm, composed of serial links, is introduced in this paper. To provide maximum range of human motion, several redundant joints are added to the serial links. In order to reduce the number of joints to be measured, kinematics of serial links was taken into consideration in design. Three measurable, controllable joints and three redundant free joints are used for the upper arm (shoulder), similarly to the forearm (wrist) while one measurable, controllable joint is used for the elbow. In particular, a torque sensor beam is designed for fine force reflection using the strain gauge. It detects the torque as well as its direction applied by the human operator, which allows the electric brake to be used as an actuator for force reflection. The electric brake constrains the joint movement so that the operator can feel the force. This electric brake outperforms the motor in terms of torque/weight ratio and makes the device light and compact. This masterarm measures the movement of the operator's arm precisely, and it can be used for teleoperation with a slave robot, or as a motion planner for an industrial robot.

1 Introduction

Robots don't have sufficient capabilities to perform complex tasks unless it is completely autonomous. Numerous studies have been done over the years on the robot teleoperation to make it possible for a supervisor to command the robot from a remote site monitoring the interaction of the robot with its environments [1]. In addition to teaching capability, the operator can have more realistic interaction with the environment by providing feedback. There is an obvious need to use feedback from widely differing sensors in or-

der to properly monitor various aspects of the task, especially for complex tasks. For teleoperated object manipulation, force and vision feedback are the most important sensing modes. Vision is useful for aligning objects, while force ensures reasonable contact forces are maintained as parts mating occurs. In force reflecting master-slave systems, forces are measured at the slave and transmitted to the master system. Since the pioneering work of [2], who developed several teleoperation systems for nuclear application, a number of similar systems and schemes have been proposed. In recent years, the feedback of tactile and kinesthetic sensory input has been suggested for the application in virtual reality technology. The interest in force feedback systems for virtual reality applications has led to the development of many systems, ranging from force reflecting joysticks to whole force feedback arm-exoskeletons [3][4]. Most of the exoskeleton-type masterarms have a kinematic design similar to that of the slave arm, with actuators, usually electric motors, thus making the masterarm bulky and heavy. [5] introduced the exoskeleton-type masterarm with pneumatic actuators, which is very light and compact but requires compressed air supply to implement force feedback. Teleoperation with motion capturing devices was introduced [6], which generates the slave robot's motion command from the partitioned inverse kinematics, showing that the masterarm's kinematic structure doesn't have to be the same as the slave robot's. [7] introduced the distributed controller architecture, which makes the efficient allocation of control, sensing, communication tasks as well as simple wiring for better implementation and maintenance possible. In this paper, a new exoskeleton-type masterarm with force reflection based on torque sensor beam is presented. To provide maximum range of the operator's movement, several redundant joints were included and iterative design analysis was performed to reduce the number of joints to be measured. After design simulation, three measurable, controllable joints and three redundant free joints are selected for the upper arm (shoulder), similarly to the forearm (wrist) while one

---

*patents pending

[†]Visiting Scientist, Department of Electrical Engineering, University of Washington, Seattle, WA

[‡]Assistant Professor, Department of Mechanical Engineering, Texas A&M University, College Station, TX

measurable, controllable joint is used for the elbow. In addition, calibration algorithm is given to compensate the variation of the kinematic parameters. For the force reflection, an electric brake is used instead of an electric motor. This electric brake constrains joint movements so that the human operator can feel the force. In particular, a torque sensor beam is designed for fine force reflection using the strain gauge. It can detect the torque as well as its direction applied by the human operator, and this allows the electric brake to be used as an actuator for the force reflection. The electric brake outperforms the motor in terms of torque/weight ratio by making the device light and compact and the operator feels less than 3 kg of weight on his arm. In the following section, the kinematic design and analysis for the proposed masterarm is described. Calibration is introduced and verified in section 3. The design concept and experimental results of force reflection based on the torque sensor beam are given in section 4, followed by a conclusion.

2 Kinematic Design and Analysis

In designing the masterarm, the following points were taken into consideration.

- the masterarm's joint angle is to be measured directly rather than by using position/orientation sensors in Cartesian coordinates.

- movement of the operator who wears the masterarm should not be constrained by the joint limit or collision with links of the masterarm.

- To achieve the maximum coverage of the operator's movement, extra redundant joints may be added, if necessary.

- Even with redundant joints, less number of joints with encoders is preferred for simple hardware implementation.

- Singular configuration should be avoided.

- Each joint should have an actuator for force feedback

Using 3D graphic modeling/simulation package, various designs of the masterarm is testified. Various combinations of the joint types, either revolute or prismatic, and link parameters were tested. Similar simulation was performed for the wrist part. The final optimal design is as follows.

- 3 measurable/controllable joints + 3 free joints for shoulder.

- One measurable/controllable joint for elbow.

- 3 measurable/controllable joints + 3 free joints for wrist.

The final design of the masterarm is shown in Figure 1. For shoulder, the first three joints have an encoder plus electric brake module, and the rest three are free joints. Without measuring the free joints, the movement of the arm can be completely calculated, which is described in the following in detail. The master-
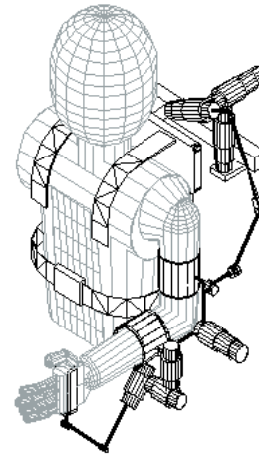

Figure 1: Exoskeleton-type Masterarm

arm coordinates are defined as shown in Figure 2. As previously mentioned, the first three joints are measurable, but the rest three joints are not. The upper arm forward kinematics is defined as getting the location where the shoulder of the masterarm is fixed at the upper arm from the first three measurable joint angles. The following assumptions are used to achieve the forward kinematics.

- The locations of the shoulder and wrist center are known

- The initial location is known

- The shoulder joint is modeled as a ball-socket joint

Along with these assumptions, only the upper arm kinematics is described since that of the forearm is very similar. The first three angles (θ_1, θ_2, θ_3) are measurable and θ_4, θ_5 and θ_6 are not. First, θ_4 can be derived by finding the intersection point of two spheres as described in Eqs. (1) and (2).

$$x^2 + y^2 + z^2 = l_5^2 + l_6^2 \qquad (1)$$

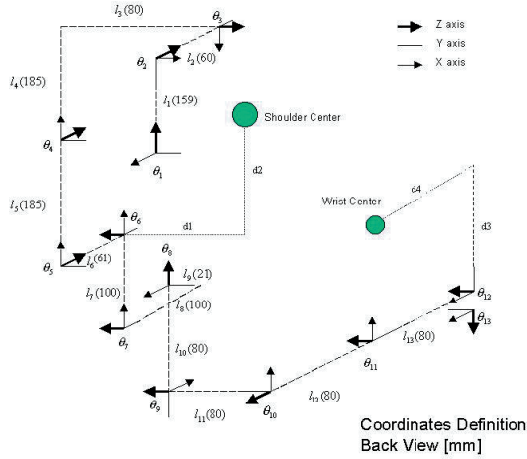$$(x - P_{4x})^2 + (y - P_{4y})^2 + (z - P_{4z})^2 = d_1^2 + d_2^2 \qquad (2)$$

Figure 2: Masterarm Coordinates

where (P_{4x}, P_{4y}, P_{4z}) is the shoulder center point looked at from the origin of θ_4's coordinates, O_{ls4}. The intersection point, A, is located on the dotted circle as shown in Figure 3. Let the point, A be (x_4, y_4, l_6) , then Eqs. (1) and (2) becomes

$$x_4^2 + y_4^2 = l_5^2 \tag{3}$$

$$(x_4 - P_{4x})^2 + (y_4 - P_{4y})^2 + (l_6 - P_{4z})^2 = d_1^2 + d_2^2 \tag{4}$$

from Eqs. (3) and (4),

$$x_4 = \frac{\alpha P_{4x} \pm \sqrt{(\alpha P_{4x})^2 + (l_5^2 P_{4y}^2 - \alpha^2)(P_{4x}^2 + P_{4y}^2)}}{P_{4x}^2 + P_{4y}^2} \tag{5}$$

$$y_4 = \frac{\alpha - x_4 P_{4x}}{P_{4y}} \tag{6}$$

where

$$\alpha = \frac{P_{4x}^2 + P_{4y}^2 + l_5^2 - d_1^2 - d_2^2 + (l_6 - P_{4z})^2}{2} \tag{7}$$

One of these solutions is not real, and actual solution is

$$\theta_4 = \tan^{-1}(y_4, x_4) - \pi \tag{8}$$

Intersection point, B, can be calculated by solving Eqs. (9) and (10), and is shown in Figure 4.

$$x^2 + y^2 + z^2 = l_6^2 + d_1^2 \tag{9}$$

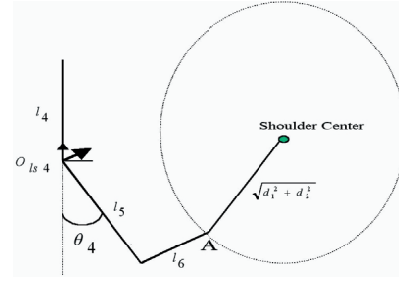$$(x - P_{5x})^2 + (y - P_{5y})^2 + (z - P_{5z})^2 = d_2^2 \tag{10}$$

Figure 3: Intersection point A

By substituting (x_5, y_5, l_6) into x, y, z respectively, the solution is derived as Eqs. (11) and (12).

$$x_5 = \frac{\beta P_{5x} \pm \sqrt{(\beta P_{5x})^2 + (d_1^2 P_{5y}^2 - \beta^2)(P_{5x}^2 + P_{5y}^2)}}{P_{5x}^2 + P_{5y}^2} \tag{11}$$

$$y_5 = \frac{\beta - x_5 P_{5x}}{P_{5y}} \tag{12}$$

where

$$\beta = \frac{P_{5x}^2 + P_{5y}^2 + l_5^2 + d_1^2 - d_2^2 + (l_6 - P_{5z})^2}{2} \tag{13}$$
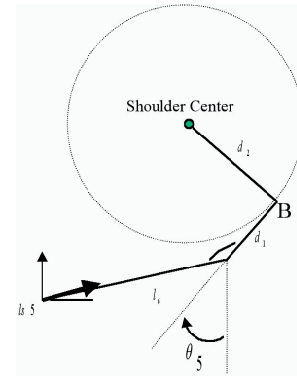
Similar to θ_4 , only one solution is valid.

Figure 4: Intersection point B

$$\theta_5 = \tan^{-1}(y_5, x_5) - \frac{\pi}{2} \tag{14}$$

Since θ_4 and θ_5 are determined, the solution of θ_6 is unique as in Eq. (15).

$$\theta_6 = \tan^{-1}(P_{6y}, P_{6x}) \tag{15}$$

where P_{6x} ,P_{6y} are x, y coordinates of shoulder center point looked at from the origin of the 6th rotational base.

3 Calibration

Analytical forward kinematics is derived in the previous section with several assumptions, but the location of the shoulder center varies depending on the operator and the location of the initial end point is not always the same. To calibrate these unknown parameters, an encoder is used to measure θ_4 only for calibration. Once those parameters are calculated from calibration, θ_4 doesn't have to be measured any more. Figure 5 shows the concept of calibration: the center of the virtual shoulder means the shoulder center point. The location of P in Figure 5 is always on the surface of a sphere centered at the virtual shoulder. The location of the virtual shoulder center and the radius of the sphere can be calculated from the least square method. In other words, various locations of P are sampled by freely moving operator's arm and then the center and radius of the sphere are calculated from the least square method. The location of the initial end point is directly calculated from assigned posture of the operator. Figure 6 shows the measured and cal-
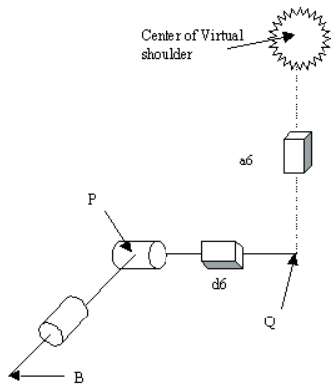

Figure 6: Measured θ_4, Estimated θ_4 without Calibration and Estimated θ_4 with Calibration

calibration algorithms are derived for the wrist part.

Figure 7: Visualization of Calibration

Figure 5: Virtual Shoulder

culated θ_4 before/after calibration, respectively. The calculated θ_4 after calibration is well matched with the measured one. The convergence of the least square method to find the center and radius is achieved only after 5 iterations with 45 data sets of P. Figure 7 shows the result of the calibration. The small spheres are the measured P locations. The large sphere's radius and center location are estimated from calibration. The operator's shoulder joint is not exactly a ball-socket joint and the joint location changes as he moves his arm. When the operator stretches or lifts the upper arm, the shoulder joint also moves. Thus the calculated virtual center/radius only produces the least amount of error, but not zero. This calibration algorithm is verified using the real ball-socket joint and various sampled points of P are located exactly on a sphere after calibration. Similar kinematics and
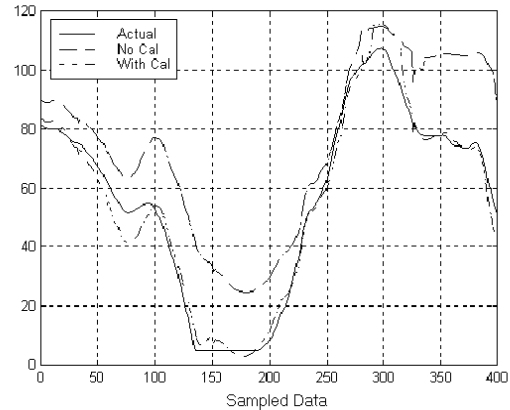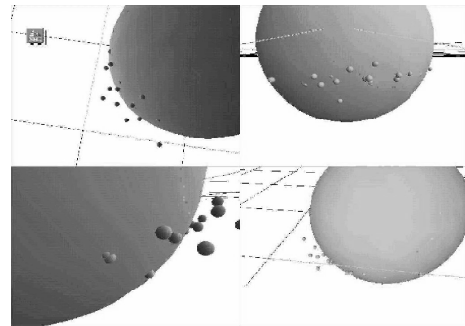
4 Force Reflection based on Torque Sensor Beam

4.1 Design and Analysis

Electric motors have been widely used as actuators for force reflection of exoskeleton-type masterarms. A torque sensor, so called *torque sensor beam* throughout this paper, using strain gauge is designed to allow an electric brake to be used as the actuator for force reflection. It is necessary that the torque sensor beam has the capabilities to detect both torque and its direction applied by the human operator. Each measurable/controllable joint module is composed of an encoder (A), electric brake (B), gear head (C), torque sensor beam (D), and cover with link (E) as shown in Figure 8. The encoder is used to measure the joint angle, and the electric brake is to constrain the joint motion with the applied torque. Once the electric brake is

activated, the torque and its direction can be sensed from the torque sensor beam. In case the operator wants to move his arm toward the opposite direction of the applied torque, the electric brake is released so that he can move freely. Figure 9 shows the calibration result of the torque sensor beam (moment versus strain gauge voltage).
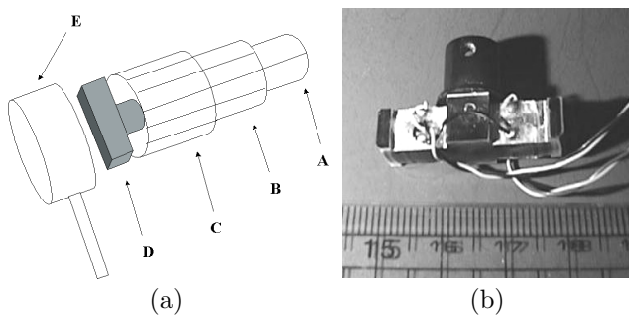

(a)   (b)

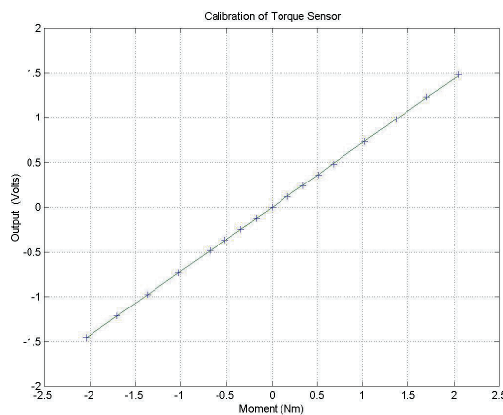Figure 8: Joint Module and Torque Sensor Beam

Figure 9: Calibration Result of the Torque Sensor Beam

4.2 Integration with Virtual Environment

This masterarm is integrated with a real robot and virtual environment. Trajectory commands are generated as human moves his arm and at the same time, the force information is fed back to the masterarm controller for force reflection. The force imposed to the robot is measured by the force/torque sensor attached at its wrists or the torque sensor at each joint. The measured force is converted to the force command to masterarm. The distributed controller architecture [7] is used for the masterarm. The torque applied to the

human operator is based on the following equations

$$\tau = \mathbf{J}_m^T(\theta)\mathbf{F}_s \qquad (16)$$

where $\mathbf{J}$; masterarm's Jacobian
$\mathbf{F}_s$; nx1 slave robot's force/moment vector
τ ; 13x1 masterarm's joint torque vector

This masterarm is integrated with a virtual environment using graphics, too. For simplicity, the first wrist joint, θ_8 is integrated with VE. The schematic diagram for the experiment is composed of three parts as shown in Figure 10 : free motion regime (I), contact regime (II), and virtual wall regime (III). The motion of the masterarm is restricted by the initial force sent from VE in the contact regime (II). As long as the contact is being kept, the force can be increased or decreased proportionally to the amount of the torque sensed by the torque sensor beam. When only the torque smaller than the initial offset(note that this is different from the initial force) is sensed, the opposite direction is detected and thus the electric brake is released so that the operator can move freely. Figure 11 shows the experimental result, and the trajectories are angle (a), PWM command (b), and torque signal (c) respectively. The contact regime was set at 20 degree.
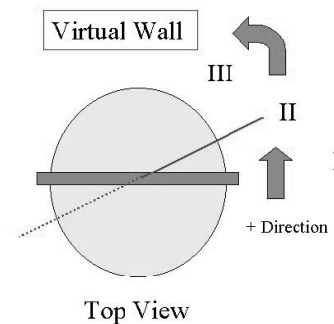
Once contacted, the force is fed back to the mas-

Figure 10: Experiment

terarm to activate the electric brake and at the same time. The initial offset(the dotted line, (c)) for detecting the opposite direction is set. During the contact, we can see that the PWM command(the solid line, (b)) decreases(from 50 to 0, note that torque generated from the brake is inversly proportional to PWM command) and increases (from 0 to 50) proportionally according to the torque amount sensed by the torque sensor beam: the difference between the sensed torque signal(the solid line, (c)) and the initial offset(the dotted line, (c)) is reflected to control the electric brake. When the torque smaller than the initial offset (169)
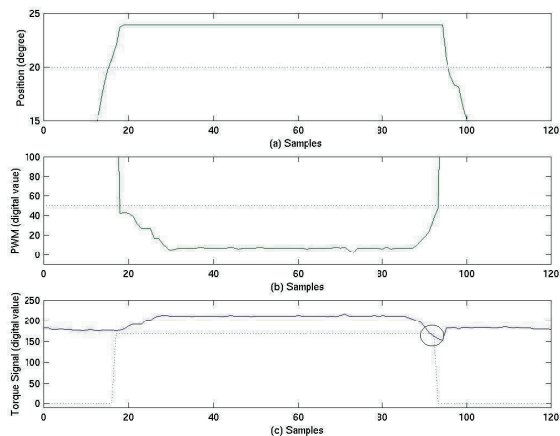
Figure 11: Experiment Result

is sensed(the circle of (c)), the opposite direction(from II to I) is detected and thus the electric brake is released(the PWM command becomes 255). This simple experimental result shows clearly that the force applied to a human operator can be increased or decreased proportionally to the torque amount sensed by the torque sensor beam. In other words, this masterarm based on the torque sensor beam allows the operator to feel the same force during the contact without the numerical computation which causes difficulties in determining visco-elastic parameters. With this proposed masterarm, we can freely design the force as the virtual robot interacts with the environment and the force reflection can make the operator feel as if he moves toward to an object with a particular shape and grasp it.

5 Conclusion

A new exoskeleton-type masterarm with force reflection based on the torque sensor beam is presented. In this paper, large working range is achieved by adding several redundant free joints. The operator's movement can be calculated without measuring the free joints, which reduces the number of necessary joints with encoders. Calibration algorithm is developed and verified. For force reflection, electric brakes are used as actuators instead of electric motors based on the torque sensor beam by detecting the torque and its direction. The electric brake outperforms the motor in terms of torque/weight ratio: the operator feels less than 3 kg of weight on his arm with the lighter and more compact device. Therefore, this proposed masterarm can be used for teleoperation with a slave robot as well as a motion planner for an industrial robot.

References

[1] T. B. Sheridan, *Telerobotics, Automation and Human Supervisory Control* The MIT Press, Cambridge, MA

[2] R. Goertz, *Manipulator Systems Development at ANL*, Proc. 12th Conf. On Remote Systems Technology, American Nuclear Society, vol. 12, 1964

[3] J. W. Hill, J. F. Jensen, P. S. Green, A. S. Shah, *Two-Handled Telepresence Surgery Demonstration Systems*, Proc. ANS Sixth Annual Topical Meeting on Robotics and Remote Systems, 1995

[4] M. Bergamasco, B. Allotta, L. Bosio, L. Ferretti, G. Parrini, G. M. Prisco, F. Salesdo, G. Sartini, *An Arm Exoskeleton System for Teleoperation and Virtual Environments Applications*, IEEE Int. Conf. On Robotics and Automation, pp. 1449-1454, 1994

[5] S. Lee, S. Park, M. Kim, C.-W. Lee, *Design of a Force Reflecting Master Arm and Master Hand using Pneumatic Actuators*, IEEE Int. Conf. on Robotics and Automation, pp. 2574-2579, 1998

[6] S. Lee, D. Choi, M. Kim, C.-W. Lee, J.-B. Song, *An Unified Approach to Teleoperation : Human and Robot Integration*, IEEE/RSJ Int. Conf. on Intelligent Robots and Systems, pp. 261-266, 1998

[7] S. Lee, J. Lee, D. Choi, M. Kim, C.-W. Lee, *The Distributed Controller Architecture for a Masterarm and its Appication to Teleoperation with Force Feedback*, IEEE Int. Conf. on Robotics and Automation, pp. 213-218, 1999